IN SITU ANALYSIS OF THE H ISOTOPE COMPOSITION OF WATER IN THE MATRIX OF UNEQUILIBRATED ORDINARY CHONDRITES.

H. Grant[1], R. Tartèse[1], L. Piani[2], R. H. Jones[1], Y. Marrocchi[2]. [1]Department of Earth and Environmental Sciences, The University of Manchester, Manchester, M13 9PL, UK (helen.grant@postgrad.manchester.ac.uk), [2]CRPG, CNRS, Université de Lorraine, UMR 7358, Vandoeuvre-lès-Nancy, 54501, France.

Introduction: The leading model for the origin of volatile species such as water, carbon, and nitrogen on Earth is through accretion from small Solar System bodies (SSSBs) that formed early in the formation of the Solar System [e.g. 1-2]. A thorough understanding of their volatile inventory, in particular of volatiles hosted in the porous fine-grained matrix found between larger high temperature components such as chondrules and CAIs is, therefore, crucial. Water-bearing minerals in the matrix of the least metamorphosed ordinary chondrites (OCs) [e.g. 2-4] provide evidence for the occurence of aqueous alteration in their asteroidal parent bodies [5]. Our recent work on the bulk water content and H isotope composition of a comprehensive set of unequilibrated OCs (UOCs) with petrological subtypes 3.00-3.9 [6] is consistent with earlier studies that showed both evidence for fluid-rock interactions [2-4] and unusually high D/H ratios in the least metamorphosed samples [e.g. 2, 7-9]. Such elevated D/H ratios in UOCs are particularly unexpected as their parent bodies are believed to have formed in the D-poor inner Solar System [10-11]. However, components other than water, such as organic compounds, may also contribute to bulk D/H ratios, which may not be fully representative of water D/H ratios. To investigate water-specific D/H ratios further, we have carried out *in situ* H isotope analysis in the fine-grained matrix of 13 of the most pristine UOC falls.

Samples and Methods: *In situ* analyses were carried out on the matrices of the following 13 UOC samples, all of which are falls: Aba Panu, Bishunpur, Bremervörde, Ceniceros, Chainpur, Krymka, Mezö-Madaras, Ngawi, Parnallee, Semarkona, Sharps, St Mary's County, and Tieschitz. Samples include all groups and petrologic subtypes ranging from 3.00 to 3.9. Millimeter-sized chips were polished using SiC polishing discs and isopropyl alcohol as the lubricant, followed by 6, 3, and 1 µm diamond pastes. Polished chips were then mounted in indium.

Electron probe microanalysis (EPMA) was carried out using the Cameca SX 100 and JEOL 8200 instruments at the University of Manchester and the University of New Mexico, respectively, to provide quantitative bulk matrix chemical compositions. Analyses were performed with an accelerating voltage of 15 kV, a beam current of 20 nA, and a 10 µm diameter defocused beam.

Prior to secondary ion mass spectrometry (SIMS) analyses, the mounts were re-polished, left overnight in an 80°C furnace to remove any adsorbed water, then gold coated and introduced to the instrument vacuum system several days before analysis. The vacuum during analysis was always $< 5\times10^{-9}$ mbar. A 10 keV Cs^+ beam was focused to a spot size of 15 × 15 µm on the same matrix regions where we did EPMA analyses, and intensities of ^{1}H, ^{2}D, ^{13}C, and ^{29}Si were measured in monocollection mode using the Cameca IMS 1280HR2 instrument at CRPG Nancy (see [12] for further details).

Results: *Matrix composition* – For each sample, four to eight areas were analyzed, depending on the availability of large, fine-grained, well-polished matrix regions suitable for EPMA. Average oxide totals varied from ~82 wt% for Chainpur (LL3.4) up to 101 wt% for Aba Panu (L3.6).

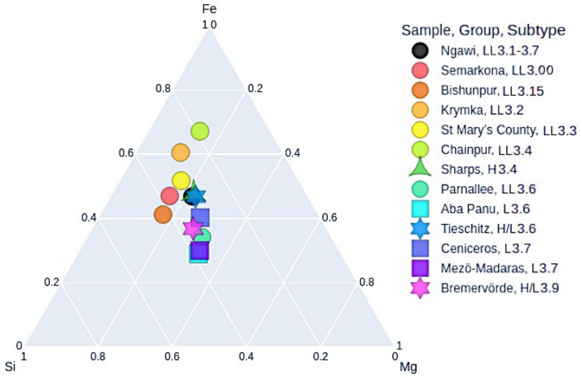

Figure 1: Fe-Mg-Si ternary plot showing average matrix compositions for each sample.

The Mg-Fe-Si ternary plot (Fig. 1) shows a general decrease in Si and increase in Fe with increasing petrologic subtype within the LL group, and variations of Fe and Mg abundances between groups for the same petrologic subtypes. There appears to be a general trend of decreasing Fe with increasing subtype; however, this may be a sampling artefact as samples of the lowest subtypes are all LLs.

Matrix D/H and C/H ratios – The samples display significant D/H and C/H variations, within and between samples (Fig. 2). Matrix areas in Semarkona, Ngawi, and Bishunpur have the largest spread of D/H ratios, with δD values ranging between *ca*. -300 and +9500‰ (where the mean of Earth ocean water is at δD = 0‰; Fig. 2). The highest δD values, measured in Semarkona (LL3.00) and Ngawi (a breccia with

LL3.1-3.7 lithologies [13]) are similar to the highest values measured in the matrix of Semarkona by [9]. The remaining 10 samples have lower matrix D/H, with δD values ranging between *ca*. -300 to +2000‰ (Fig. 2).

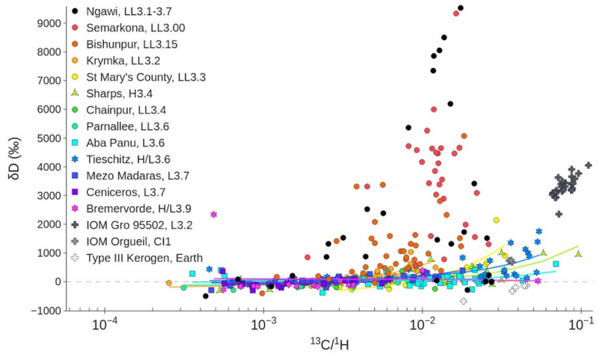

Figure 2: δD vs. $^{13}C/^{1}H$ for UOC matrix analyses, including reference samples. Colored lines are linear regressions for petrologic subtypes > 3.2. The grey dashed line represents the Earth ocean mean δD.

Overall, the spread and average matrix δD values decrease with increasing petrologic subtype, with the exception of Tieschitz (LL3.6) which displays a large spread of δD values for its subtype (Fig. 3).

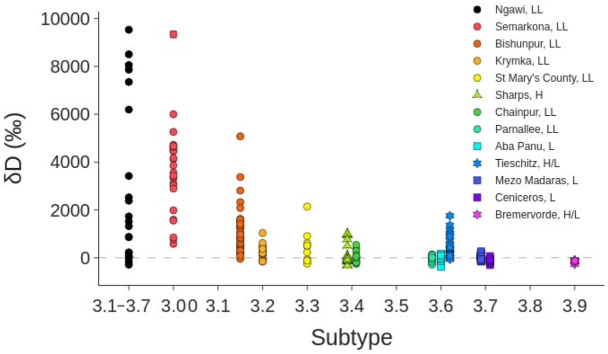

Figure 3: Matrix δD values vs. petrologic subtype (samples with the same subtypes offset for clarity).

Discussion: Major element oxide totals summed to less than 95 wt% in many samples with subtypes <3.6, which may be attributed to hydrated phyllosilicates, C-rich phases, and porosity. There is a general increase in oxide totals with increasing subtype, suggesting a decrease in water- and/or C-rich material in UOC matrix with increasing thermal metamorphism, in agreement with previous studies [e.g. 4, 6].

Estimations of contributions from organic or hydrated phases in fine-grained matrix SIMS analyses can be approximated by comparing C/H and D/H ratios. For chondrites displaying linear correlations between measured D/H and C/H, the y-axis intercept at C/H = 0 (i.e. no organic contribution) provides an estimate of the water D/H ratio [e.g. 12]. Samples with petrologic subtypes ≥3.2 display linear correlations (displayed as curves in Fig. 2 as the $^{13}C/^{1}H$ axis uses a log scale) between (i) C-rich organic components with δD values of up to *ca*. +2000‰, typical for UOC insoluble organic matter (IOM) [9, 14], and (ii) C-free water end-members with δD values of *ca*. -350 to -100‰, similar to CM chondrite water δD values [12].

The D/H vs. C/H relationship in the matrix of Semarkona (LL3.00), Bishunpur (LL3.15) and Ngawi (LL3.1-3.7) is less evident, with most matrix analyses plotting in a triangle between (i) C-rich / moderate δD IOM, (ii) C-free / low δD water, and (iii) high δD values with intermediate C/H ratios. This component with intermediate C/H ratios is characterized by extremely high δD values of up to almost +10000‰. On the other hand, the D/H ratios of their H-rich, C-poor components, inferred to be water, is similar to that of more metamorphosed UOCs and CM chondrites. The D-rich matrix component with intermediate C/H ratios is not apparent in samples with subtypes ≥ 3.2, suggesting that it is not very resistant to even mild thermal metamorphism. This is in stark contrast to the thermally resistant D-rich component of UOC IOM [e.g. 14].

These results suggest that the OC parent bodies may not have accreted ices with D/H ratios higher than those accreted by CC parent bodies from the outer protoplanetary disc, alleviating a major conundrum of current protoplanetary disc water transport models [10-11]. The component with extremely high D/H identified in the least metamorphosed UOCs is neither phyllosilicate nor IOM, but instead a previously unidentified D-rich phase.

Acknowledgments: We acknowledge the UK STFC and Europlanet 2024 for funding, and the Natural History Museum (London), the American Museum of Natural History (NYC), and the Smithsonian Institution (Washington DC) for loans of the samples studied.

References: [1] Broadley M et al. (2022) *Nature*, 611: 245–255. [2] Alexander C. M. O'D. et al. (2012) *Science*, *337*, 721-723. [3] Dobrica E. & Brearley A. J. (2014) *Meteoritics & Planet. Sci.*, *49*, 1323-1349. [4] Alexander C. M. O'D. et al. (1989) *EPSL*, *95*, 187-207. [5] Jin Z. & Bose M. (2019) *Sci. Adv.*, *5*, eaav8106. [6] Grant H. et al. (2022) *MetSoc*, Abstract #6342. [7] McNaughton N. et al. (1982) *LPSC XIII*, A297-A302. [8] Robert F. and Merlivat L. (1979) *Nature*, *282*, 785-789. [9] Piani L. et al. 2015. *EPSL* 415: 154–164. [10] Yang L. et al. (2013) *Icarus*, *226*, 256-267. [11] Jacquet E. and Robert F. (2013) *Icarus*, *223*, 722-732. [12] Piani L. et al. (2021) *EPSL*, 567, 117008. [13] Grossman J. N. & Brearley A. J. (2005) *Meteoritics & Planet. Sci.* 40: 87–122. [14] Remusat L. et al. (2016) *EPSL* 435: 36–44.